


Ultralong TE In Vivo ^1H MR Spectroscopy of Omega-3 Fatty Acids in Subcutaneous Adipose Tissue at 7 T

Martin Gajdošík, PhD,^{1,2,3}  Lukas Hingerl, MSc,¹ Antonín Škoch, MD, PhD,^{4,5} Angelika Freudenthaler, MS,² Patrik Krumpolec, PhD,^{1,6} Jozef Ukropec, PhD,⁶ Barbara Ukropcová, MD, PhD,⁶ Petr Šedivý, PhD,⁵ Milan Hájek, PhD,⁵ Bianca K. Itariu, PhD,² Bernhard Maier, MD,⁷ Sabina Baumgartner-Parzer, PhD,² Michael Krebs, MD,² Siegfried Trattnig, MD,^{1,8} and Martin Krššák, PhD^{1,2,8*}

Background: Omega-3 (n-3) fatty acids (FA) play an important role in neural development and other metabolic diseases such as obesity and diabetes. The knowledge about the in vivo content and distribution of n-3 FA in human body tissues is not well established and the standard quantification of FA is invasive and costly.

Purpose: To detect omega-3 (n-3 CH_3) and non-omega-3 (CH_3) methyl group resonance lines with echo times up to 1200 msec, in oils, for the assessment of n-3 FA content, and the n-3 FA fraction in adipose tissue in vivo.

Study Type: Prospective technical development.

Population: Three oils with different n-3 FA content and 24 healthy subjects.

Field Strength/Sequence: Single-voxel MR spectroscopy (SVS) with a point-resolved spectroscopy (PRESS) sequence with an echo time (TE) of 1000 msec at 7 T.

Assessment: Knowledge about the J-coupling evolution of both CH_3 resonances was used for the optimal detection of the n-3 CH_3 resonance line at a TE of 1000 msec. The accuracy of the method in oils and in vivo was validated from a biopsy sample with gas chromatography analysis.

Statistical Tests: SVS data were compared to gas chromatography with the Pearson correlation coefficient.

Results: T_2 relaxation times in oils were assessed as follows: CH_2 , 65 ± 22 msec; CH_3 , 325 ± 7 msec; and n-3 CH_3 , 628 ± 34 msec. The n-3 FA fractions from oil phantom experiments ($n = 3$) were in agreement with chromatography analysis and the comparison of in vivo obtained data with the results of chromatography analysis ($n = 5$) yielded a significant correlation ($P = 0.029$).

Data Conclusion: PRESS with ultralong-TE can detect and quantify the n-3 CH_3 signal in vivo at 7 T.

Level of Evidence 1

Technical Efficacy Stage 1

J. MAGN. RESON. IMAGING 2019;50:71–82.

OMEGA-3 (ω -3 or n-3) fatty acids (FA), together with n-6 FA, are essential polyunsaturated FA important for humans. n-3 FA are involved in neural development^{1,2} and could be part of a novel therapy for nonalcoholic fatty liver disease (NAFLD).³ Today, several invasive methodologies enable the quantification of n-3 FAs; however, these methods are

View this article online at wileyonlinelibrary.com. DOI: 10.1002/jmri.26605

Received Oct 12, 2018, Accepted for publication Nov 28, 2018.

*Address reprint requests to: M.K., Division of Endocrinology and Metabolism, Department of Medicine III, Medical University of Vienna, Währinger Gürtel 18-20, A-1090 Vienna, Austria. E-mail: martin.krssak@meduniwien.ac.at

From the ¹High-field MR Centre, Department of Biomedical Imaging and Image-guided Therapy, Medical University of Vienna, Vienna, Austria; ²Division of Endocrinology and Metabolism, Department of Internal Medicine III, Medical University of Vienna, Vienna, Austria; ³Bernard and Irene Schwartz Center for Biomedical Imaging, Department of Radiology, New York University School of Medicine, New York, New York; ⁴National Institute of Mental Health, Klecany, Czech Republic; ⁵MR Unit, Department of Diagnostic and Interventional Radiology, Institute for Clinical and Experimental Medicine, Prague, Czech Republic; ⁶Institute of Experimental Endocrinology, Biomedical Research Center, Slovak Academy of Sciences, Bratislava, Slovakia; ⁷University Clinic for Trauma Surgery, Medical University of Vienna, Vienna, Austria; and ⁸Christian Doppler Laboratory for Clinical Molecular MR Imaging, Vienna, Austria

This is an open access article under the terms of the Creative Commons Attribution-NonCommercial License, which permits use, distribution and reproduction in any medium, provided the original work is properly cited and is not used for commercial purposes.

time-consuming and costly.^{4,5} Knowledge about the in vivo content and distribution of n-3 FA in human body tissues is not well established.

Proton (¹H) nuclear magnetic resonance (NMR) spectroscopy enables the detection of terminal protons of n-3 methyl (n-3 CH₃) and non-n-3 methyl (CH₃) groups in FA chains at two different frequencies (ν): 0.98 and 0.90 ppm.⁶⁻⁸ The methyl protons are coupled to two protons on the second carbon atom and form triplets in the NMR spectra. In the case of the n-3 CH₃ group, the J-coupling constant is 7.5 Hz.⁹ The relatively adjacent base frequencies and signal splitting make the detection of n-3 FA in vivo challenging. The in vivo fraction of n-3 FA from the total FA chain is very low, ~1:75 in adipose tissue.⁹ This complicates its detection and prolongs signal acquisition times.

As signal-to-noise (SNR) increases with magnetic field strength (B₀), ultrahigh field (UHF) 7 Tesla (T) should provide higher SNR, which is beneficial for the detection of low-concentration n-3 FA. The nominal spectral resolution in Hz between CH₃ and n-3 CH₃ increases with the application of higher B₀; however, the resolution of the methyl triplets remains constant. For a better understanding of this effect, the estimated spectral dispersion in vivo is illustrated in Fig. 1 for three clinical field strengths of 1.5, 3, and 7 T.

At magnetic field strengths of 1.5 and 3 T, the peaks of the CH₃ triplet overlap the central and right outer n-3 CH₃ peaks; however, no signal overlaps the left outer n-3 CH₃ peak (1.08 ppm and 1.05 ppm, respectively) and can, in principle, be detected. The first detection of n-3 FA in vivo in subcutaneous adipose tissue (SAT) at a clinical field strength of 1.5 T with ¹H MR spectroscopy (MRS) was carried out by Lundbom et al.,¹⁰ in which the left outer n-3 CH₃ peak was detected using a point-resolved spectroscopy (PRESS) sequence¹¹ with a long echo time (TE) of 540 msec. This in vivo n-3 FA measurement was based on a long apparent transverse (T₂) relaxation time of 478 msec for the central n-3 CH₃ peak of linseed oil measured in that study. A method for assessment of the relative levels of n-3 FA content in oils, based on relative methyl peak linewidths with stimulated echo mode (STEAM) and PRESS sequences with TE = 160 msec at 3 T, was also presented.¹² J-difference editing allowed for the detection of the left outer n-3 CH₃ peak in SAT at 1.05 ppm with a TE of 199.5 msec at 3 T.⁹ However, at 7 T the left outer n-3 CH₃ peak resonates at 1.00 ppm, which is only 0.02 ppm away from the central n-3 CH₃ peak. To detect this peak with in vivo MRS in SAT using a whole-body 7 T MRI system and the usual B₀ homogeneity is currently very difficult.

Nevertheless, the spectral dispersion at 7 T yields a better resolution of the central peaks of both methyl triplets, which have two-times higher intensity than their respective outer peaks.

All the aforementioned MRS methods used a medium TE (≥ 160 msec) that exploits the relatively long T₂ relaxation times of

n-3 methyl groups compared to the neighboring non-n-3 methyl groups and strong methylene ((CH₂)_n or CH₂) peak (3-5 \times longer), which resonates at a frequency close to 1.30 ppm.^{10,13} However, MRS measurements with a long TE have the disadvantage of heavy T₂-weighting, which requires an accurate description of J-modulation and the calculation of T₂ relaxation times for the correct assessment of the FA content.^{14,15} The effect of J-coupling interactions on the quantification and assessment of the T₂ relaxation time of the CH₃ group has been investigated in oils and bone marrow at 3 T with TE ≤ 200 msec.¹⁵

MRS at UHF is generally hampered by a higher specific absorption rate (SAR) and a larger chemical-shift-displacement error (CSDE). These obstacles can be overcome at the cost of worse localization and longer acquisition time by using Hermite pulses,¹⁶ which have lower RF power requirements, and by measuring with specific frequency offsets.¹⁷

The aim of this study was to detect and characterize the relaxation behavior of CH₂, CH₃, and n-3 CH₃ signals in oils, with an assessment of their apparent T₂ relaxation times and their n-3 FA content, and to detect and quantify n-3 CH₃ signal in vivo in SAT with a long TE at 7 T. For this purpose, we aimed to modify the PRESS sequence for UHF and validated the MRS data by gas chromatography analysis.

Materials and Methods

Theoretical Considerations for n-3 CH₃-specific Echo Timing

FAs have long aliphatic chains, which can contain ~10-30 carbons. The simulation of their relaxation behavior presents a complex problem. As Lundbom et al.¹⁰ pointed out, methylene and methyl protons at the end of non-n-3 FA chains are weakly coupled ($\Delta\nu \gg J$), which allows for an approximation using a CH₃ spin system.⁹ J-modulation of outer lines (S) of the n-3 CH₃ triplet can then be described as a function of TE:

$$S(TE) = S_{xy} \cos(2 * \pi * J * TE) \exp(-TE/T_2) \quad (1)$$

where S_{xy} represents the transverse magnetization of the outer triplet n-3 CH₃ protons and J is the coupling constant (7.5 Hz).

Considering the limited B₀ homogeneity in in vivo MRS, the outer triplet lines of n-3 CH₃ in antiphase may improve the spectral resolution of the central lines of CH₃ and n-3 CH₃ signals. Due to the expected low n-3 FA content in vivo, the n-3 CH₃ signal acquired with TE < 200 msec will be overlaid by strong and broad signals from the CH₂ and CH₃ groups. Thus, TEs longer than 200 msec shall be used to detect the n-3 CH₃ signal. As proposed by Škoch et al.,⁹ the TEs for the measurements of the outer triplets in antiphase can be simply calculated according to:

$$TE = \frac{1}{J} \left(\frac{1}{2} + k \right) \quad (2)$$

where k = 0, 1, 2, 3,.... According to this function, the first eight applicable TEs ≥ 200 msec for n-3 CH₃ detection will be: 200, 335,

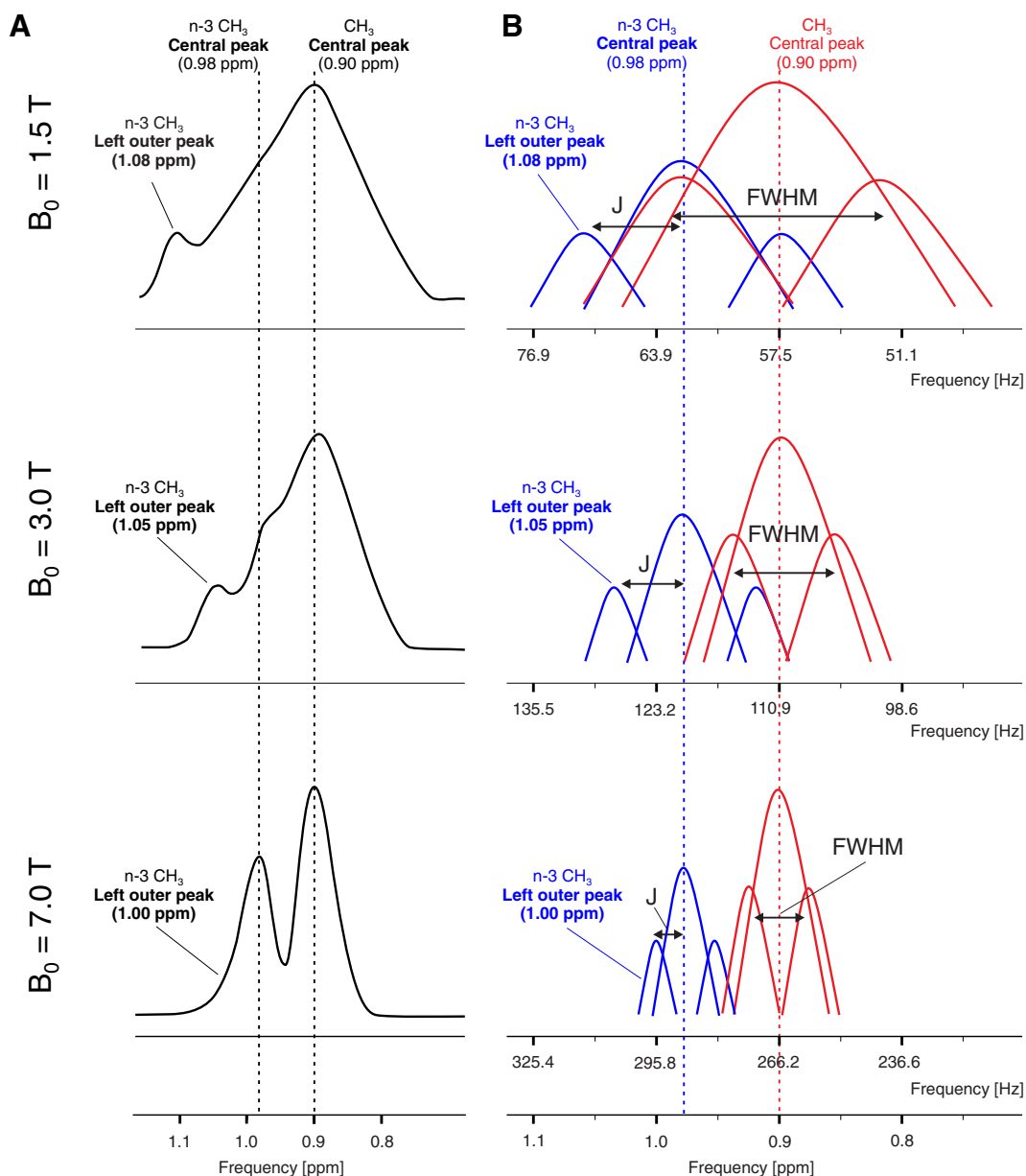


FIGURE 1: Illustration of different spectral dispersions for n-3 CH₃ and CH₃ spectra for three different magnetic field strengths (scaling of absolute frequency adapted to respective field strength) and CH₃ linewidths expected in in vivo experiments (spectral linewidth ~14 Hz) (A). Note the better separation of the n-3 CH₃ left outer peak at 1.5 T and the better separation of the central peaks at 7 T. Two properties of MR play a role in the different separations of the n-3 CH₃ and CH₃ signals: the J-coupling constant, which retains the chemical shifts of the triplets constant; and the Larmor frequency, which better separates the triplets with an increase of B₀ (B).

470, 600, 735, 865, 1000, and 1130 msec. The simulation of the T₂ relaxation behavior of CH₂ and CH₃ protons with apparent T₂ relaxation times of the CH₂, CH₃, and n-3 CH₃ groups measured in oils¹⁰ with an estimated n-3 FA in vivo content is depicted in Fig. 2. As shown in the simulations, the shortest TE for n-3 CH₃ detection with a negligible CH₂ signal occurrence would be 1000 msec (ultralong TE).

Due to an imperfect signal quantification, B₀ inhomogeneity, and the complicated J-modulations of all lipid resonances, the calculated relaxation times should not be considered as true, but rather, as apparent T₂ relaxation times.^{10,15} For the sake of simplicity, we will use the term T₂ (relaxation) times for measured apparent T₂ relaxation times.

RF Pulse Profiles for 7 T and n-3 CH₃ Simulations

The frequency profiles of the excitation and refocusing RF pulses in the standard PRESS sequence (Sinc pulse with duration = 2.6 msec, Mao pulse with duration = 6.0 msec¹⁸) and excitation and refocusing Hermite pulses (excitation duration = 2.6 msec, refocusing duration = 3.0 msec) were measured in a silicone oil phantom using a birdcage extremity coil at 7 T, with a spin echo sequence and frequency encoding in the slice-encoding direction (transversal slab; thickness, 20 mm; field of view [FOV], 400 × 400 mm; TE = 230 msec; TR = 5 sec; bandwidth [BW] = 10 kHz).

The n-3 CH₂-CH₃ spin system was simulated and verified with a pulse acquired sequence with a 2 msec rectangular pulse and TE < 1 msec in the NMRScope-B tool in the jMRUI package.^{19,20}

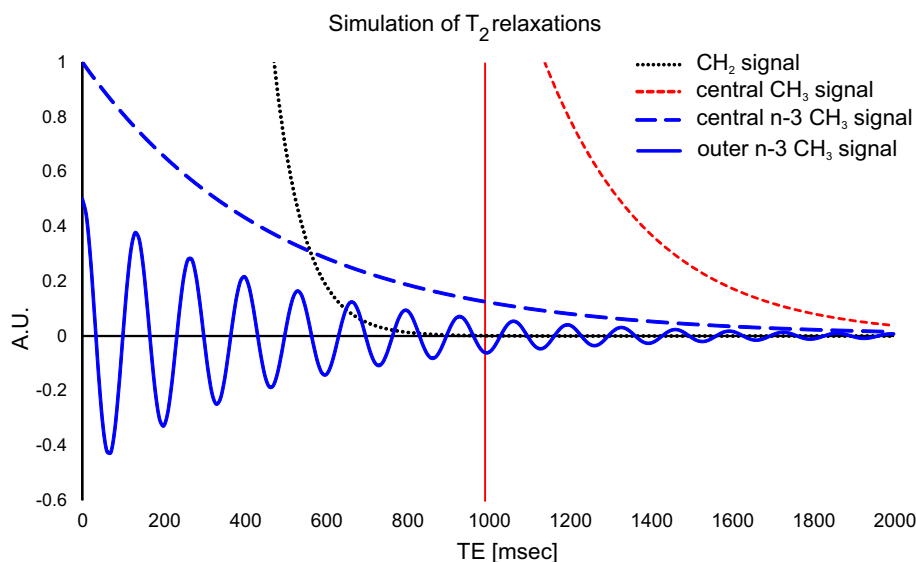


FIGURE 2: Simulations of T_2 relaxations for the CH_2 group (black), the central CH_3 peak (red), and the central n-3 CH_3 peak with the outer triplet n-3 CH_3 peak (blue). The simulated T_2 relaxations were calculated with a concentration of n-3 FA of 1:75 and with the following T_2 relaxation times: CH_2 , 76 msec; CH_3 , 264 msec, mean values from several oils; and n-3 CH_3 , 478 msec measured in linseed oil. These T_2 relaxation times from oils were obtained from Ref. 10. According to the simulations, at TE = 1000 msec, there will be a negligible occurrence of the CH_2 signal with still more than 10% of the n-3 CH_3 signal intensity. Data were normalized to the central n-3 CH_3 peak intensity at TE = 0 msec.

The symmetric PRESS sequence with Hermite pulses and RF pulses centered at 1 ppm was simulated with TEs of 30 (shortest TE for PRESS) and 1000 msec (ultralong TE) for one spin, to replicate the effect of RF pulse bandwidths with ideal localization, and a 1 mL isotropic voxel, for realistic RF pulse effects and localization.

MR Hardware and Spectroscopy Sequence

All MRS measurements were performed on a 7 T Magnetom scanner (Siemens Healthineers, Erlangen, Germany) with a 28-channel knee coil (Quality Electrodynamics, Mayfield Village, OH).

The spectroscopic voxel was positioned according to T_1 -weighted scout images. The frequency was adjusted on the CH_2 signal at 1.3 ppm and the homogeneity of the B_0 field was first improved with automatic B_0 shimming calculated from gradient echo images, then manually adjusted in an interactive mode. The reference voltage for RF pulses was automatically calibrated by the scanner. A frequency offset of -0.3 ppm was used for all measurements.

The PRESS sequence was equipped with the same Hermite pulses and durations as in the simulation. The signal was acquired with 2048 complex points and the receiver bandwidth was set to 3000 Hz.

Oil Phantoms

The oil measurements were performed on three samples with different n-3 FA content: Menhaden fish oil (high n-3 FA content), soybean oil (medium n-3 FA content), and corn oil (low n-3 FA content) (Sigma-Aldrich, St. Louis, MO, USA). The oils were poured into small plastic spheres (\varnothing 38 mm) and measured at room temperature.

The spectra for the assessment of the T_2 relaxation times were measured from a volume of interest (VOI) of 0.5 mL with 60 TEs

in a range of 30–1200 msec, with echo steps of 20 msec, TR = 5 sec, and number of acquisitions (NA) = 6.

In Vivo Measurements

The study protocol was approved by the Institutional Review Board and the Ethics Committee and written, informed consent was obtained from all participants prior to the study. In vivo MRS measurements were performed on 24 healthy subjects (14 females / 10 males, mean age: 35.7 ± 12.8 years, range: 26–68 years; mean body mass index: 24.7 ± 5.8 $\text{kg}\cdot\text{m}^{-2}$, range: 18.8–49.5 $\text{kg}\cdot\text{m}^{-2}$). Except for two subjects on a vegetarian diet, none of the volunteers had any other dietary restrictions.

The typical VOI was set to 8 mL and placed in the SAT in the lower part of the thigh. The voxel was positioned just above the knee (3–4 cm), so the knee was at the inferior edge of the coil and the axial scout image was in the center. The in vivo spectra were measured with ultralong TE = 1000 msec, TR = 5 sec, and NA = 32.

SAT Biopsy

Five samples taken from the same anatomical SAT region measured with MRS were further analyzed by gas chromatography–mass spectrometry (GC-MS). Whole SAT samples from the knee region were obtained from three subjects who underwent either elective liposuction of the legs or elective arthroscopy of the knee joint. Subjects were excluded if they presented with leg ulcers or soft-tissue infection of the legs or suffered from any relevant systemic disease that would exclude patients from local anesthesia. SAT biopsies were performed at the end of the procedures, shortly before suture, by cutting a piece of SAT that did not exceed 3 g, or ~ 1 cm^3 , from a site along the incision line at the front of the knee. Samples from another two subjects were obtained under local anesthesia by the Bergström technique, as described in detail previously.²¹ All samples

were immediately snap-frozen and stored at -80°C until GC-MS analysis.

Gas Chromatography–Mass Spectrometry

About 1–2 mg of oil or tissue was homogenized in a 500 μl methanol:chloroform 1:2 solution. Each sample was spiked with C19:0 FA as an internal standard and lipids were extracted according to Folch et al.²² Lipid extracts were evaporated under a gentle stream of nitrogen. Then the samples were derived in 2 ml methanol:toluene 4:1 with 200 μl acetyl chloride at 100°C by continuous stirring. After 60 minutes, the samples were cooled to 4°C and 5 ml of 6% potassium carbonate solution was added. After centrifugation, the toluene layer was collected and used for GC-MS analysis.

A 6890 N/59730 N GC-MSD system (Agilent, Santa Clara, CA, USA) with a DB-23 30 m-column was used. Helium was used as a carrier gas with 1.0 ml/min flow in a solvent vent modus using a PTV-injector with a 250°C injection temperature. The initial oven temperature of 50°C was held for 4 minutes, then increased to 180°C at a rate of $10^{\circ}\text{C}/\text{min}$ and held for 5 minutes, which was subsequently increased to 240°C at a rate of $5^{\circ}\text{C}/\text{min}$ and held for 2 minutes and finally increased to 250°C at a rate of $3^{\circ}\text{C}/\text{min}$.

The mass spectrometer was run in the electron impact mode where the FA were detected in a scan mode of m/z 33–400. The source temperature was set to 230°C , the quadrupole temperature to 150°C , and the transfer line temperature was 260°C .

MRS Data Postprocessing and Analysis

The CH_2 , CH_3 , and $n-3$ CH_3 signals were quantified in jMRUI with the AMARES algorithm.²³ In oils, only the CH_2 peak and central peaks of the methyl triplets were fitted with a single Gaussian line (oil prior knowledge). The T_2 relaxation times were calculated in MATLAB (MathWorks, Natick, MA, USA), with the following monoexponential fitting function:

$$S(TE) = S_0 \exp(-TE/T_2) \quad (3)$$

where S_0 represents the signal (magnetization) at $TE = 0$ msec. The coefficient of determination (R^2) was used as an indicator of the quality of the fit.

In vivo, the CH_2 and central $n-3$ CH_3 peak were fitted with single Gaussian lines and the CH_3 peak was fitted with two Gaussian lines (in vivo prior knowledge). Since the J-modulation of the CH_3 group was unknown, outer triplet CH_3 peaks were approximately fitted with a second Gaussian line to minimize a possible influence on the quantification of the relatively small $n-3$ CH_3 peak.

Spectral quality was estimated according to the full width at half maximum (FWHM) of the CH_2 signal measured at $TE = 30$ msec ($\text{FWHM}_{\text{CH}_2}$), the FWHM of the CH_3 signal measured at $TE = 1000$ msec ($\text{FWHM}_{\text{CH}_3}$), and SNR, calculated as the ratio of the CH_3 signal amplitude measured at $TE = 1000$ msec to the last 200 points of free induction decay. Exclusion criteria for in vivo spectra were a $\text{FWHM}_{\text{CH}_3} > 30$ Hz and $\text{SNR} < 15$.

The $n-3$ FA content in oils was calculated as the ratio of the $n-3$ CH_3 signal to the sum of both methyl signals measured with $TE = 1000$ msec after the T_2 relaxation correction:

$$n-3 \text{ FA content} = \frac{I_{n-3\text{CH}_3, T_2}}{I_{\text{CH}_3, T_2} + I_{n-3\text{CH}_3, T_2}} \times 100\% \quad (4)$$

where I_{CH_3, T_2} and $I_{n-3 \text{CH}_3, T_2}$ are the signal intensities after correcting for T_2 relaxation, and are given in percent. To test in vivo prior knowledge, the $n-3$ FA content in oils was also calculated from line-broadened spectra adjusted to in vivo spectral quality.

The in vivo $n-3$ FA fraction in SAT (in arbitrary units) was calculated according to:

$$n-3 \text{ FA fraction} = \frac{I_{n-3\text{CH}_3}}{I_{\text{CH}_3} + I_{n-3\text{CH}_3}} \quad (5)$$

where I_{CH_3} and $I_{n-3\text{CH}_3}$ are the signal intensities measured with $TE = 1000$ msec, and are given in arbitrary units (a.u.).

Quantification of FA with GC-MS was performed by correlating the integrated peak areas of FA with the integrated area of C19:0, which was used as an internal standard. The $n-3$ FA content by GC-MS was calculated as the ratio of $n-3$ FA to total FA. In vivo MRS data were compared to GC-MS with the Pearson correlation coefficient. All data are reported as the mean \pm standard deviation (SD) and $P < 0.05$ was considered statistically significant. The amplitudes of MRS signals are shown in a.u.

Results

RF Pulses and Sequence Simulations

The experimentally measured FWHM of the Sinc pulse was 3.4 kHz and the Mao pulse was 1.1 kHz. The FWHMs of the excitation and refocusing Hermite pulses were 1.6 kHz and 1.1 kHz, respectively. The flat frequency range of both Hermite pulses was ~ 500 Hz (1.7 ppm at 7 T). The frequency profiles of all RF pulses are shown in Fig. 3A,B. Accounting for the center of the RF pulses (1.0 ppm), this range covered nearly all the relevant chemical shifts of methylene and methyl protons, which is depicted in Fig. 3C. The simulation of the $n-3$ methyl group with the pulse acquired sequence confirmed our spin model, and is shown in Fig. 3D. The simulated imperfections of the Hermite pulses and PRESS localization are depicted in Fig. 3E,F for TEs of 30 and 1000 msec, respectively.

Detection of $n-3$ CH_3 and T_2 Relaxation in Oil Phantoms

The spectral triplet pattern of the CH_3 and $n-3$ CH_3 groups was clearly visible in the observed region by the application of a properly adjusted long TE in all oil phantoms. Reference spectra showing CH_2 , $n-3$ CH_3 , and CH_3 signals from all three oils measured with $TE = 30$ and 1000 msec are depicted in Fig. 4. The $n-3$ CH_3 signals in the measured spectra were in agreement with the simulations.

The maximum FWHM in all oils for the central CH_3 peak was < 4.5 Hz and, for the central $n-3$ CH_3

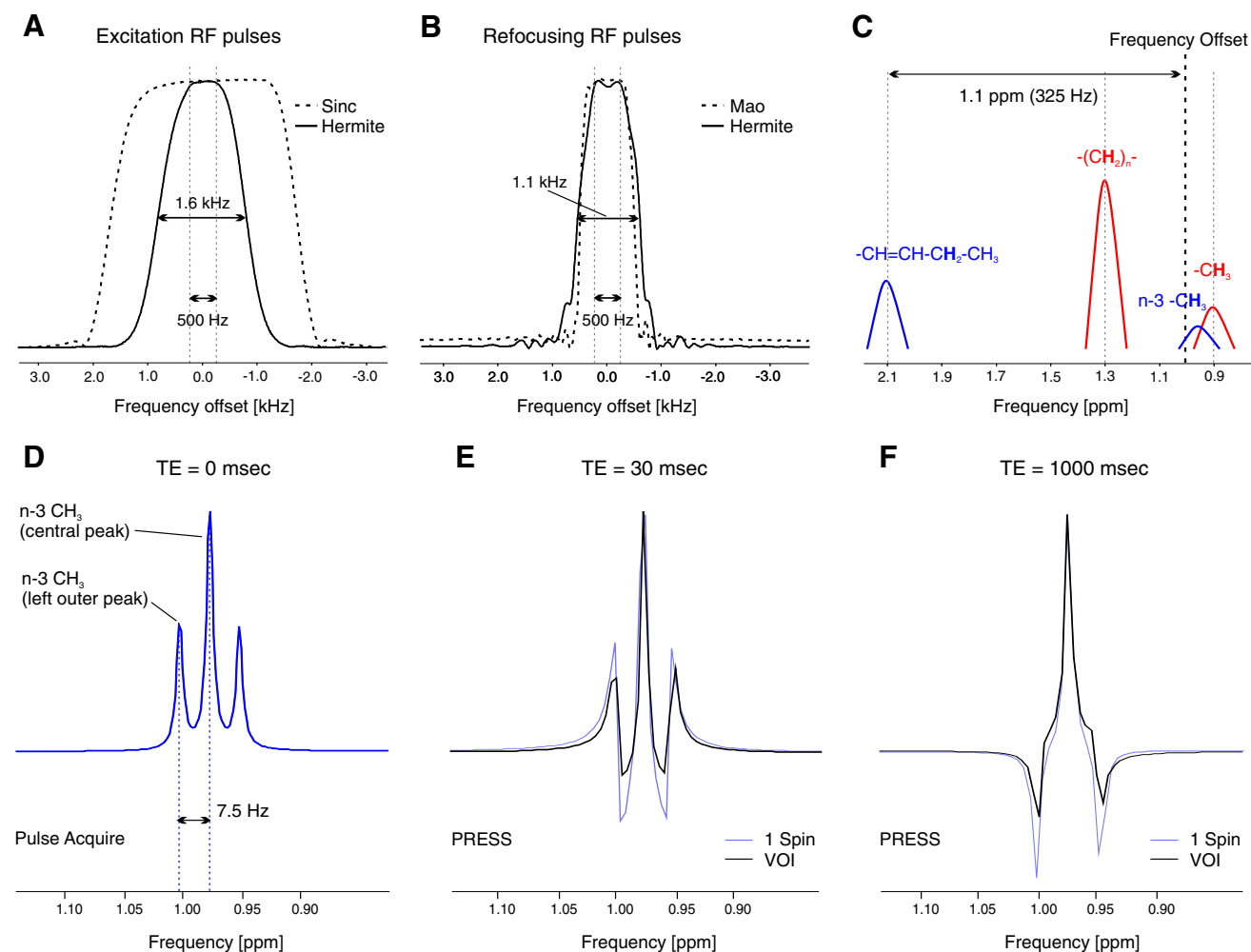


FIGURE 3: Excitation and refocusing bandwidth of Sinc and Hermite pulses measured in phantoms (A,B) (500 Hz = 1.7 ppm at 7 T). Both excitation and refocusing pulses in the PRESS sequence used in this study could excite and refocus methylene and methyl protons in the n -3 FAs (blue) and the non- n -3 FAs (red) (C). The spin system of the n -3 CH_3 used for simulation was demonstrated with a pulse acquire sequence (rectangular pulse with a duration of 2 msec) (D). The effects of standard Mao and Hermite pulses for one spin and for a VOI of 1 mL, respectively, were simulated for short and ultralong TEs (E,F). All simulations were apodized with a 2 Hz Lorentzian filter.

peak, <3.2 Hz. The T_2 relaxation of all central peaks was influenced by the J-modulation from the outer triplet peaks.

The measured T_2 relaxation behavior of the CH_2 group, as well as the central signals of the CH_3 and n -3 CH_3 groups for the three oil samples, with calculated T_2 times for the CH_3 groups, are depicted in Fig. 5. The T_2 relaxation times of the all groups together with their R^2 values are shown in Table 1.

Detection of n -3 CH_3 In Vivo

The thighs of all subjects fit easily in the knee coil except for one case, when the MRS had to be performed in SAT in the calf due to an excessive amount fat in the thigh ($\text{BMI} \sim 50 \text{ kg}\cdot\text{m}^{-2}$). A typical localization of a voxel in the SAT is depicted in Fig. 6A,B. The spectral quality for the detection of the n -3 CH_3 signal was sufficient in all volunteers; however, in two cases the very small

amount of SAT in very lean and athletic males forced a doubling of the number of acquisitions. The n -3 CH_3 resonance, measured with ultralong TE and $\text{NA} = 32$, was clearly resolved in vivo with the advantage of the suppression of the strong CH_2 signal, as depicted in Fig. 6C. Signal fitting with Gaussian line-shapes yielded an acceptable fit with minimal residual signals, as shown in Fig. 6D.

The mean $\text{FWHM}_{\text{CH}_2}$ in vivo was 26.9 ± 4.0 Hz, the $\text{FWHM}_{\text{CH}_3}$ for CH_3 was 13.3 ± 4.1 Hz, and, for n -3 CH_3 was 11.5 ± 2.4 Hz. The mean SNR was 159 ± 111 . There was no significant correlation found between the $\text{FWHM}_{\text{CH}_3}$ and SNR.

Based on the mean values of the $\text{FWHM}_{\text{CH}_3}$ measured from in vivo spectra, a line-broadening using a 12 Hz Gaussian filter was applied on oil spectra measured with a TE of 1000 msec. The mean $\text{FWHM}_{\text{CH}_3}$ after the line-broadening for CH_3 was 13.4 ± 1.0 Hz, and for n -3 CH_3 was

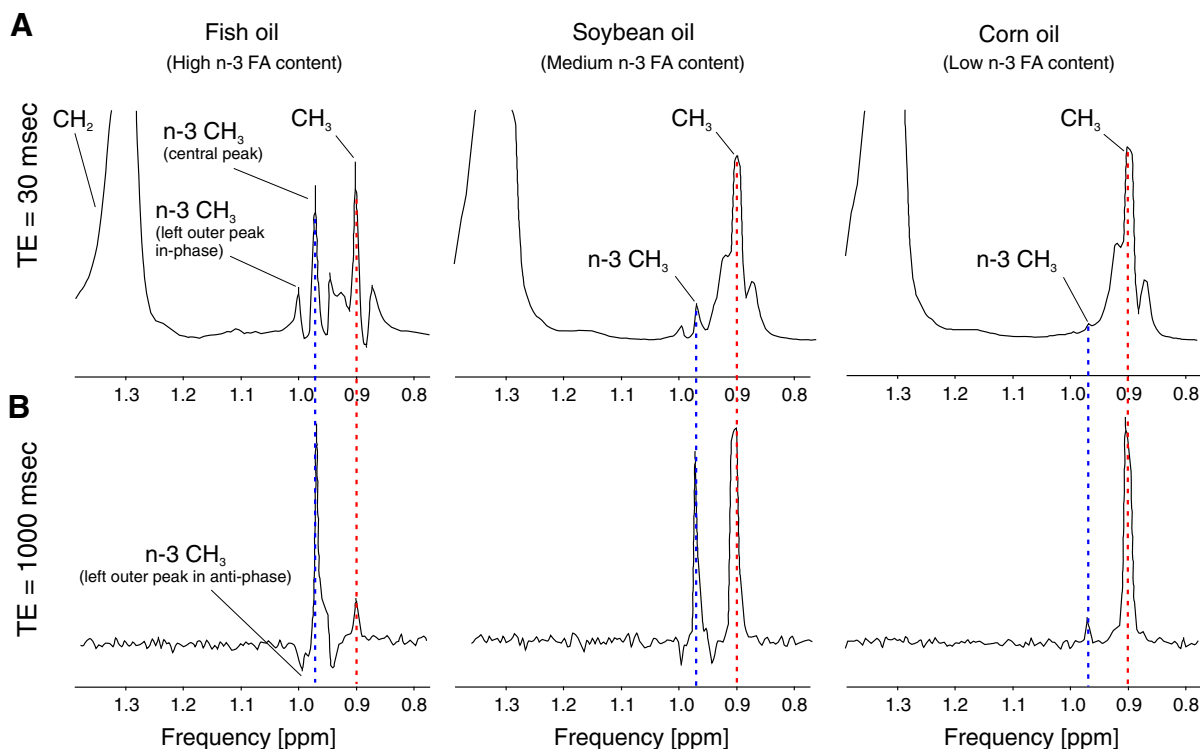


FIGURE 4: Spectra from three oils with different n-3 FA content measured with a short TE = 30 msec (A) and an ultralong TE = 1000 msec (B). The FWHM of the CH₃ signal in the oils measured with a TE = 30 msec was ~5 Hz.

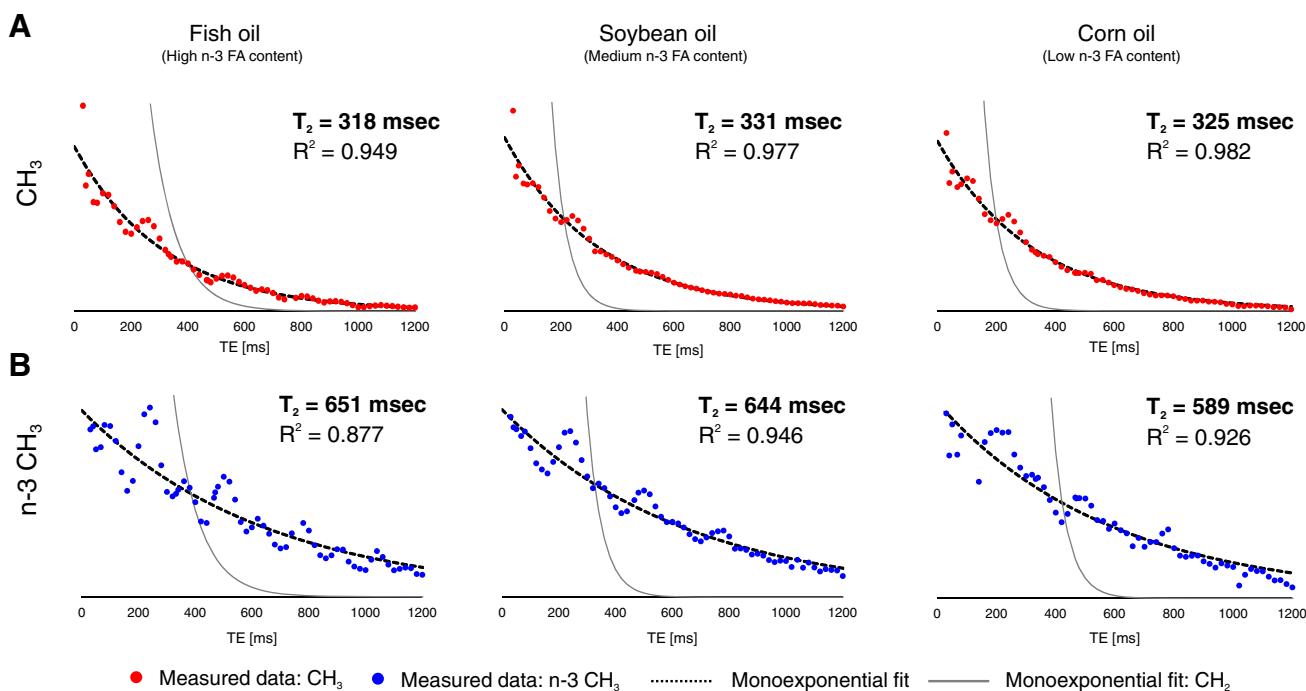


FIGURE 5: T₂ relaxation behavior and T₂ relaxation times of the central CH₃ peak (A) and the central n-3 CH₃ peak (B) from three oil samples with different n-3 FA content. All signals were fitted with monoexponential functions (dashed lines). For comparison of T₂ relaxations, the measured CH₂ data from the corresponding oils are shown as a solid gray line.

11.0 ± 0.1 Hz. The example of a soybean oil spectrum before and after line-broadening, together with fitting with oil prior knowledge and in vivo prior knowledge, is depicted in Fig. 6E,F, respectively.

Quantification and Validation of the n-3 FA Content in Oils and the n-3 FA Fraction in SAT

The n-3 FA content in oils yielded a high correlation with data from the GC-MS analysis, which is shown in

TABLE 1. Individual T₂ Relaxation Times of CH₂, CH₃, and n-3 CH₃ Groups in Oils and Mean T₂ Relaxation Times in Oils and In Vivo

	T ₂ : CH ₂ [msec]	R ² : CH ₂	T ₂ : CH ₃ [msec]	R ² : CH ₃	T ₂ : n-3 CH ₃ [msec]	R ² : n-3 CH ₃
Fish oil	90	0.996	318	0.949	651	0.877
Soybean oil	53	0.990	331	0.977	644	0.946
Corn oil	51	0.992	325	0.982	589	0.926
Oils (<i>n</i> = 3)	65 ± 22	0.993 ± 0.003	325 ± 7	0.969 ± 0.018	623 ± 34	0.916 ± 0.036

All T₂ relaxation times are shown with individual and mean R² values.

Fig. 7A. The oil spectra after line-broadening correlated with GC-MS as well (Fig. 7B).

The n-3 FA fractions in vivo from all volunteers ranged from 0.085–0.252 and the mean fraction was 0.149 ± 0.042 . The mean n-3 FA fraction in females (*n* = 14) was 0.140 ± 0.036 , ranging from 0.085–0.228, and in males (*n* = 10) was 0.161 ± 0.046 , ranging from 0.111–0.252. This difference was found to be not significant. No significant correlations were found between age, BMI, and n-3 FA fraction (in a.u., without T₂ correction).

All five volunteers chosen for the SAT biopsy tolerated the procedure well. The calculated n-3 FA fractions from the SAT biopsy yielded significant correlation with the data from the GC-MS analysis (*P* = 0.029), and is depicted in Fig. 7C.

Discussion

A single-voxel PRESS sequence with TEs up to 1200 msec was used to detect n-3 CH₃ in three oil samples with different n-3 FA fractions, and in vivo. An ultralong TE of 1000 msec, high spectral resolution, and an SNR of 7 T magnetic field enabled the detection of the n-3 CH₃ signal in all three oil samples with different n-3 FA content and in the SAT of all 24 healthy subjects as well. In the presented work, the T₂ relaxation behavior of the non-n-3 and n-3 CH₃ groups was investigated in oils, with an assessment of their apparent T₂ relaxation times. The calculated n-3 FA content in oils and n-3 FA fractions in vivo were validated by GC-MS analysis.

The spin-echo-based ¹H PRESS single-voxel method is the sequence of choice due to its wide availability on MR systems. It provides higher SNR than the STEAM²⁴ and requires less power than semi-LASER²⁵ or LASER.²⁶ In addition, PRESS is more sensitive to J-coupling than STEAM²⁷; therefore, it has been used for n-3 FA detection in previous studies as well. Due to the increased SAR demands on 7 T, we used Hermite excitation and refocusing pulses,^{16,17} which require less power at the cost of a relatively narrow bandwidth.

The PRESS sequence is sensitive to chemical shift displacement error, which increases with B₀. The Δν between the CH₂ and the CH₃ group is 0.4 ppm and between the n-3 CH₂ and the n-3 CH₃ group is 1.1 ppm, which makes the chemical shift displacement error relatively small. For the typical 8 mL cubical voxel, the displacement in one direction would be ~12% and ~33%, respectively. This relates to "four-compartment" chemical shift artifacts, which could decrease the spectral quality.²⁸ This could explain the lower intensity of the outer n-3 CH₃ signals in antiphase, as expected, by a 1:2:1 ratio with the central signal of the triplet, which was shown in the simulations. The frequency offset of the RF pulses could also be adjusted on the methylene resonance at 1.3 ppm or even further, eg., in the frequency between n-3 CH₂ and n-3 CH₃ (1.5 ppm), but, as the results of our prior experiments with oil phantoms have shown, this did not improve the spectral quality.

A spectral editing approach in SAT with oMEGA-PRESS was proposed by Škoch et al.,⁹ and later, with MEGA-sLASER by Lindeboom and de Graaf²⁹ at 3 T and 4 T. Nevertheless, these techniques depend on the J-coupling, which we aimed to minimize, and they would also require an additional calibration for 7 T applications. Another localized method that uses the natural abundance of ¹³C to detect FA in SAT at 7 T was proposed by Lindeboom and de Graaf.²⁹ This method enables the detection of several unique resonances for the assessment of FA saturation and the n-6/n-3 FA ratio, but requires a special double-tuned ¹H/¹³C coil for the heteronuclear pulse sequence.

With regard to the issue of spectral line quantification, it was shown that the use of different algorithms can lead to different analytic results.³⁰ AMARES quantification software offers an easy and robust solution for the quantification of MR signals without the simulation of metabolite basis sets, which, in the case of large molecules such as FA, could be very difficult. The ideal spectral line-shape for lipids could be characterized by the Voigt function³¹; however, this line-shape is not included in the AMARES quantification. The Voigt line-shape can be approximated by a combination of Lorentzian and

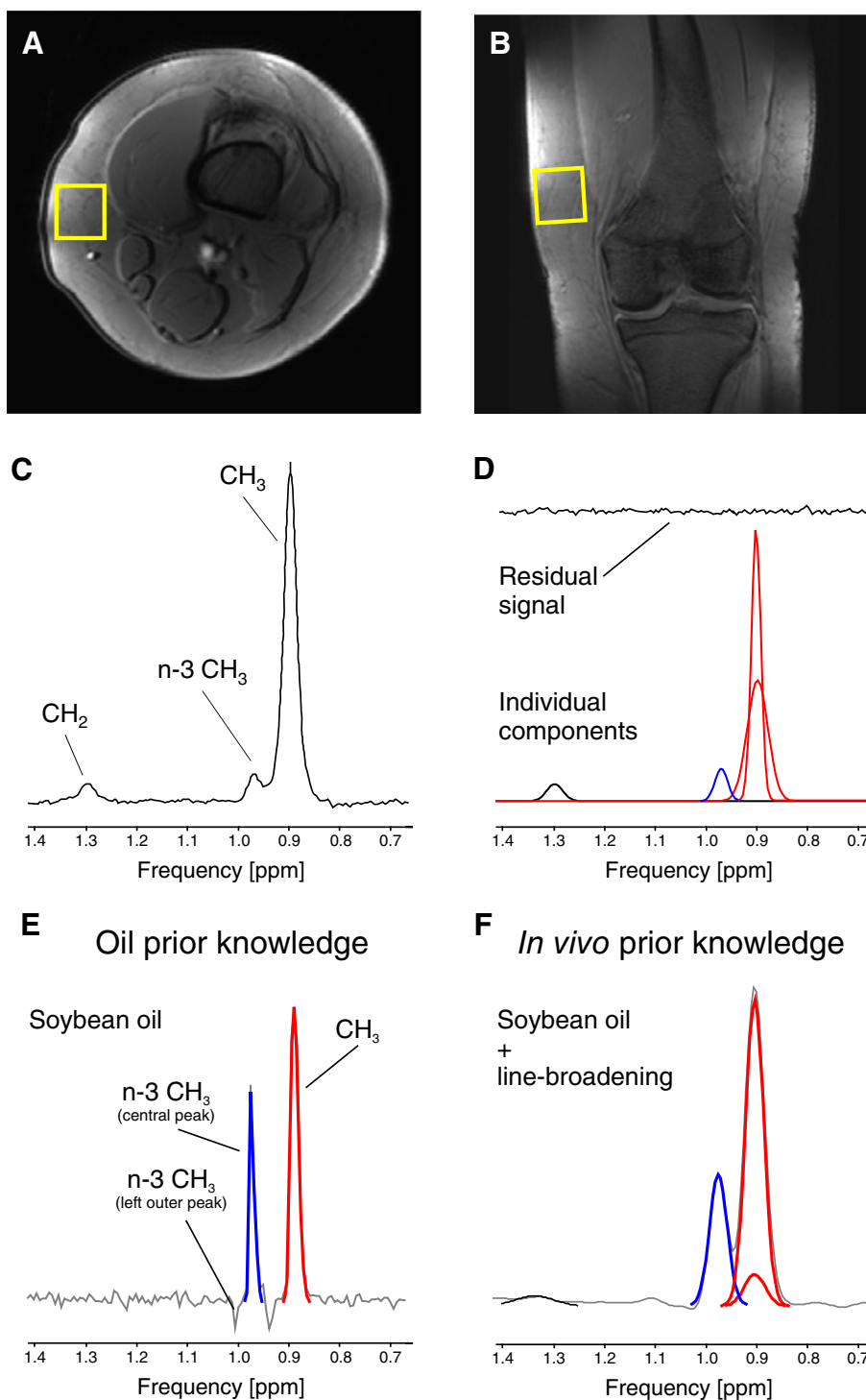


FIGURE 6: The typical position of the voxel (yellow cube) on axial (A) and coronal images (B) in SAT in a female volunteer. The corresponding in vivo proton spectrum (FWHM_{CH₃} = 9.6 Hz, SNR = 227) measured with an ultralong TE of 1000 msec and NA = 32, showed a disappearing CH₂ signal and a clear separation of the n-3 CH₃ and the CH₃ signals (C). Peak fitting of methylene and both methyl signals with Gaussian line-shapes resulted in minimal residual signals (D). An example of soybean oil spectra fitted with oil prior knowledge (two Gaussians, E) and the same spectrum with a line-broadening filter fitted with in vivo prior knowledge (three Gaussians F).

Gaussian functions. From our experience, the Lorentzian line-shape of the stronger CH₃ signal can underestimate the amplitude of the minor n-3 CH₃ signal, and using the Lorentz-Gaussian time domain filtering function may result in small, but unknown, variations in signal amplitudes.³² Instead of this

combination and filter, two Gaussian lines with a fixed frequency were used to fit the CH₃ signal and their ratio was automatically estimated by AMARES.

The magnetic field of the whole-body 7 T scanner allowed for sufficient spectral resolution of the CH₃ and n-3 CH₃ triplets

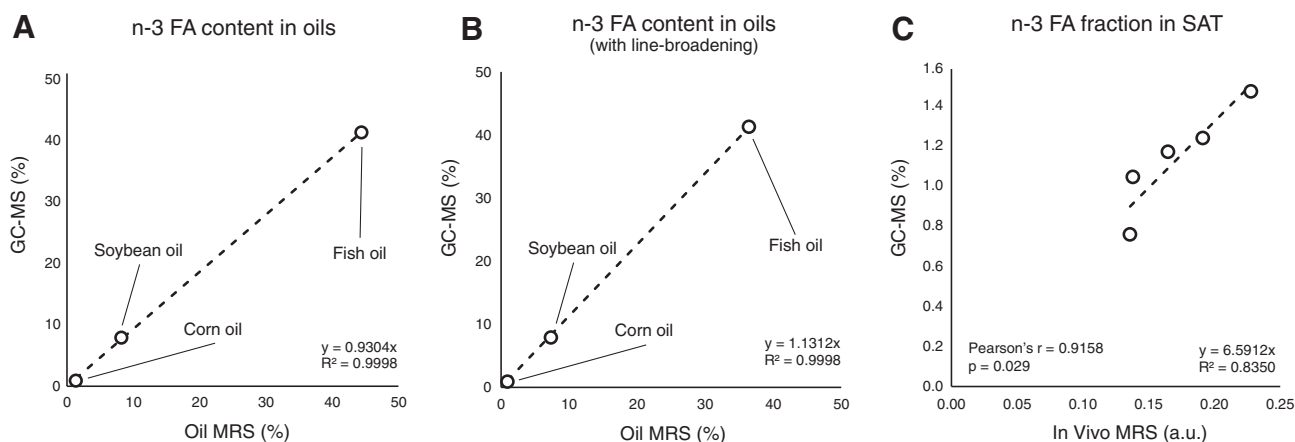


FIGURE 7: Scatterplots of the n-3 FA content in oils (A), the n-3 FA content in oils calculated from line-broadened spectra (B), and the n-3 FA fraction in subcutaneous adipose tissue (C) measured with a TE = 1000 msec and compared to GC-MS analysis.

in the oils. Our results confirmed the relatively long and different T_2 relaxation times of both methyl groups and the short T_2 relaxation times of the methylene groups, which enabled their better resolution and quantification with the ultralong TE, especially for the low n-3 FA-concentration corn oil.

J-modulations of the outer triplet peaks of the methyl groups influenced the measured T_2 decay of their central peaks; however, this effect did not hamper the calculation of the T_2 relaxation times. Because the central peaks were not affected by imperfections caused by the RF pulses and localization sequences, quantification with oil prior knowledge by fitting only the central peaks was feasible. This was demonstrated by the high correlation of their n-3 FA content with the GC-MS analysis.

The line-broadening of oil spectra caused the merging of the two methyl triplets into two partially overlapping peaks. These peaks contained signal from all the methyl protons. The quantification of the line-broadened signals with in vivo prior knowledge showed a high correlation with GC-MS analysis as well, and confirmed this approach for in vivo quantification.

The resonance frequencies of CH_3 and n-3 CH_3 are adjacent, and therefore, their distinction is extremely sensitive to B_0 field inhomogeneity. The in vivo signal measured closer to the skin experienced a slightly worse B_0 field due to the difference in magnetic susceptibility in the air-tissue boundary. In general, the FWHM of the CH_2 signal in magnitude mode during the B_0 shimming had to be less than 40 Hz in order to successfully resolve both methyl signals. Measurements with a TE of 67 msec could be chosen for n-3 CH_3 detection as well, but this would require a quite homogeneous B_0 with a small VOI (<1 mL). The suppression of the strong CH_2 signal could also be an option; however, this would require sequence optimization similar to water suppression techniques,^{33,34} which was not the aim of this study.

The assessment of n-3 FA is of great importance for understanding the metabolism of lipids. In the study by

Ouldamer et al.,³⁵ GC of FA from the SAT extracts from rats showed high correlation with ^1H MRS analysis. The n-3 FA fraction in the control group was 0.9%, and the n-3 FA content changed with dietary supplements. The n-3 FA fraction in SAT measured with in vivo MRS at 3 T has already been reported in several studies. Škoch et al.⁹ reported a content of $1.6 \pm 0.5\%$ in the dorsal waist assessed with the J-difference editing method with a TE = 199.5 msec. Lundbom et al.³⁶ reported the n-3 FA fraction in the same body area measured with TE = 540 msec in a range from 0.09–0.2%, with a range from the GC analysis of 1.0–1.8%, which represented a significant agreement ($P < 0.05$, $n = 8$). There are three n-3 FA in human lipid metabolism: α -linolenic acid (ALA, 18:3n-3); eicosapentaenoic acid (EPA, 20:5n-3); and docosahexaenoic acid (DHA, 22:6n-3), and, although the exact composition of n-3 FA would be desired, current localized ^1H MRS techniques are limited to the detection of only the n-3 CH_3 signal from the mixed content of those FAs.

Our GC-MS results, ranging from 0.8–1.5%, were in agreement with previously published data. The reported SAT n-3 FA fraction in this study should not be compared with the FA content because the signals were not corrected for T_2 relaxation. A rough estimation of n-3 FA content would be possible by using a linear regression analysis; however, this approach assumes constant T_2 relaxation times of methyl signals, which is questionable at this point. The proposed MRS method yielded a realistic validation of the aforementioned method and was in line with the literature.

Heavy T_2 -weighting of methyl signals in vivo is one important limitation of this study. Although the assessment of T_2 relaxation times of methyl groups in vivo was not the aim of this pilot study, their knowledge is critical for future research into n-3 FA using long TEs. The SAT in vivo can contain various FAs with different saturations^{37,38} and can be site-specific.³⁹ Oil phantoms are often successfully used as appropriate materials for proof-of-concept; however, for MRS measurements of subtle signals with ultralong TE, even small

variations in FA content in vivo could result in different relaxation behavior. Assessment of T_2 relaxation times with TEs < 1000 msec will pose a problem for B_0 homogeneity due to increasing overlap between CH_3 and n-3 CH_3 signals with shorter TE. There are several techniques for advanced B_0 shimming,^{40,41} which could improve the spectral resolution and allow detection of n-3 CH_3 signal with shorter TE. In addition, the T_2 times could be calculated using a monoexponential function when TEs are selected according to Eq. 2. As already mentioned, the strong CH_2 signal could be theoretically suppressed enabling using short TE (TE < 200 msec). The spectra were averaged online, which, in the case of movement of a subject, would be translated into broader linewidths. This effect can be resolved in frequency alignment and phase corrections for each transient in postprocessing in future studies. All our subjects had a sufficient layer of subcutaneous fat, but MRS in lean individuals with a small amount of fat would require very small voxels (<1 mL) and manifold NA, which could prolong acquisition time significantly. The SAT biopsy and the sample analysis is an invasive and costly technique, and, for a larger sample size, would require more time and resources, which were limited for this study. As we did not perform any test–retest measurements and we analyzed only five samples with GC-MS, further in vivo measurements of the SAT in different areas and biochemical validation from biopsy samples of a broader population are necessary.

Considering these benefits and limitations, this pilot work on direct n-3 CH_3 detection in vivo at ultrahigh fields could be very useful for preclinical studies. Because of the simplicity of this method, it can be complementary to other metabolic MRS studies of SAT, muscles, or bone marrow.

In conclusion, the differences in T_2 relaxation times between the CH_2 , CH_3 , and n-3 CH_3 signals enabled the identification of well-resolved n-3 CH_3 resonances, making PRESS with ultralong TE a method suitable for the direct detection of n-3 FA at 7 T. This work proposed a relatively simple approach for the reliable estimation of the n-3 FA fraction, in vivo, in a sample of healthy volunteers.

Acknowledgments

Contract grant sponsor: Anniversary Fund of the Austrian National Bank; Contract grant number: P15363; Contract grant sponsor: Austrian Federal Ministry of Education, Science and Research; Contract grant number: BMWFV WTZ Mobility, CZ11-2015; Contract grant sponsor: Ministry of Health of the Czech Republic; Contract grant number: MHCZ-DRO 00023001IKEM; Contract grant sponsor: Ministry of Education, Science, Research and Sport of the Slovak Republic; Contract grant number: APVV SK-AT-2017-0025 and APVV 15/0253.

The authors thank Rolf Pohmann (Max Planck Institute for Biological Cybernetics, Tübingen, Germany) for programming of the Hermite pulses, Vladimír Mlynárik and Wolfgang Bogner (Medical University of Vienna, Austria) for help with the sequence and oil experiments, and Thomas M. Stulnig and Kornelia Böhler (Medical University of Vienna, Austria) for recruitment of volunteers and assistance with tissue samples used for gas chromatography-mass spectrometry.

References

1. Amminger GP, Schäfer MR, Schlögelhofer M, Klier CM, McGorry PD. Longer-term outcome in the prevention of psychotic disorders by the Vienna omega-3 study. *Nat Commun* 2015;6:7934.
2. McNamara RK. Role of Omega-3 fatty acids in the etiology, treatment, and prevention of depression: Current status and future directions. *J Nutr Intermed Metab* 2016;5:96–106.
3. Masterton GS, Plevris JN, Hayes PC. Review article: omega-3 fatty acids — A promising novel therapy for non-alcoholic fatty liver disease. *Aliment Pharmacol Ther* 2010;31:679–92.
4. Klingler M, Koletzko B. Novel methodologies for assessing omega-3 fatty acid status — A systematic review. *Br J Nutr* 2012;107:S53–S63.
5. Messamore E, McNamara RK. Detection and treatment of omega-3 fatty acid deficiency in psychiatric practice: Rationale and implementation. *Lipids Health Dis* 2016;15:25.
6. Solladié-Cavallo A, Senouci H, Jierry L, Klein A, Bouquey M, Terrisse J. Linseed oil and mixture with maleic anhydride: 1 H and 13 C NMR. *J Am Oil Chem Soc* 2003;80:311–314.
7. Sacchi R, Savarese M, Falcigno L, Giudicianni I, Paolillo L. Proton NMR of fish oils and lipids. In: *Mod Magn Reson*. Vol. 2. Dordrecht, Netherlands: Springer; 2008:919–923.
8. Arús C, Westler WM, Bárány M, Markley JL. Observation of the terminal methyl group in fatty acids of the linolenic series by a new 1H NMR pulse sequence providing spectral editing and solvent suppression. Application to excised frog muscle and rat brain. *Biochemistry* 1986;25:3346–51.
9. Škoch A, Tošner Z, Hájek M. The in vivo J-difference editing MEGA-PRESS technique for the detection of n-3 fatty acids. *NMR Biomed* 2014; 27:1293–1299.
10. Lundbom J, Heikkinen S, Fielding B, Hakkarainen A, Taskinen M-R, Lundbom N. PRESS echo time behavior of triglyceride resonances at 1.5T: Detecting ω -3 fatty acids in adipose tissue in vivo. *J Magn Reson* 2009;201:39–47.
11. Bottomley PA. Selective volume method for performing localized NMR spectroscopy. *US Pat* 4 480 228 1984.
12. Fallone CJ, McKay RT, Yahya A. Long TE STEAM and PRESS for estimating fat olefinic/methyl ratios and relative ω -3 fat content at 3T. *J Magn Reson Imaging* 2017;1–9.
13. Lundbom J, Hakkarainen A, Söderlund S, Westerbacka J, Lundbom N, Taskinen M-R. Long-TE 1H MRS suggests that liver fat is more saturated than subcutaneous and visceral fat. *NMR Biomed* 2011;24:238–245.
14. Yahya A, Tessier AG, Fallone BG. Effect of J-coupling on lipid composition determination with localized proton magnetic resonance spectroscopy at 9.4 T. *J Magn Reson Imaging* 2011;1396:1388–1396.
15. Breitzkreutz DY, Fallone BG, Yahya A. Effect of J coupling on 1.3-ppm lipid methylene signal acquired with localised proton MRS at 3 T. *NMR Biomed* 2015;28:1324–1331.
16. Warren WS. Effects of arbitrary laser or NMR pulse shapes on population inversion and coherence. *J Chem Phys* 1984;81:5437.
17. Gajdošík M, Chadzynski GL, Hangel G, et al. Ultrashort-TE stimulated echo acquisition mode (STEAM) improves the quantification of lipids and

- fatty acid chain unsaturation in the human liver at 7T. *NMR Biomed* 2015;28.
18. Mao J, Mareci T, Andrew E. Experimental study of optimal selective 180° radiofrequency pulses. *J Magn Reson* 1988;79:1–10.
 19. Starčuk Z, Starčuková J, Štrbák O, Graveron-Demilly D. Simulation of coupled-spin systems in the steady-state free-precession acquisition mode for fast magnetic resonance (MR) spectroscopic imaging. *Meas Sci Technol* 2009;20:104033.
 20. Starčuk Z, Starčuková J. Quantum-mechanical simulations for in vivo MR spectroscopy: Principles and possibilities demonstrated with the program NMRScopeB. *Anal Biochem* 2017;529:79–97.
 21. Kurdiouva T, Balaz M, Vician M, et al. Effects of obesity, diabetes and exercise on Fndc5 gene expression and irisin release in human skeletal muscle and adipose tissue: in vivo and in vitro studies. *J Physiol* 2014; 592:1091–1107.
 22. Folch J, Lees M, Stanley, Sloane GH. A simple method for the isolation and purification of total lipides from animal tissues. *J Biol Chem* 1957; 226:497–509.
 23. Vanhamme L, van den Boogaart A, Van Huffel S. Improved method for accurate and efficient quantification of MRS data with use of prior knowledge. *J Magn Reson* 1997;129:35–43.
 24. Frahm J, Merboldt K-D, Hänicke W. Localized proton spectroscopy using stimulated echoes. *J Magn Reson* 1987;502–508.
 25. Scheenen TWJ, Klomp DWJ, Wijnen JP, Heerschap A. Short echo time 1H-MRSI of the human brain at 3T with minimal chemical shift displacement errors using adiabatic refocusing pulses. *Magn Reson Med* 2008;59:1–6.
 26. Garwood M, DelaBarre L. The return of the frequency sweep: Designing adiabatic pulses for contemporary NMR. *J Magn Reson* 2001;153: 155–177.
 27. Ernst T, Hennig J. Coupling effects in volume selective 1H spectroscopy of major brain metabolites. *Magn Reson Med* 1991;21:82–96.
 28. Kaiser LG, Young K, Matson GB. Numerical simulations of localized high field 1H MR spectroscopy. *J Magn Reson* 2008;195:67–75.
 29. Lindeboom L, de Graaf RA. Measurement of lipid composition in human skeletal muscle and adipose tissue with 1 H-MRS homonuclear spectral editing. *Magn Reson Med* 2018;79:619–627.
 30. Mosconi E, Sima DM, Osorio Garcia MI, et al. Different quantification algorithms may lead to different results: A comparison using proton MRS lipid signals. *NMR Biomed* 2014;27:431–43.
 31. Marshall I, Higinbotham J, Bruce S, Freise A. Use of Voigt lineshape for quantification of in vivo 1H spectra. *Magn Reson Med* 1997;37:651–657.
 32. Gajdošík M, Škoch A, Hájek M, Trattning S, Krššák M. Application of Lorentz-Gaussian lineshape transformation filter for improved omega-3 fatty acid quantification in thigh at 7T. In: *ISMRM Workshop on MR Spectroscopy: From Current Best Practice to Latest Frontiers*. Lake Constance, Switzerland; 2016.
 33. Ogg RJ, Kingsley RB, Taylor JS. WET, a T1- and B1-insensitive water-suppression method for in vivo localized 1H NMR spectroscopy. *J Magn Reson Ser B* 1994;104:1–10.
 34. Tkáč I, Gruetter R. Methodology of 1H NMR spectroscopy of the human brain at very high magnetic fields. *Appl Magn Reson* 2005;29:139–157.
 35. Ouldamer L, Nadal-Desbarats L, Chevalier S, Body G, Goupille C, Bougnoux P. NMR-based lipidomic approach to evaluate controlled dietary intake of lipids in adipose tissue of a rat mammary tumor model. *J Proteome Res* 2016;15:868–878.
 36. Lundbom J, Hakkarainen A, Fielding B, et al. Characterizing human adipose tissue lipids by long echo time 1H-MRS in vivo at 1.5 Tesla: validation by gas chromatography. *NMR Biomed* 2010;23:466–472.
 37. Ren J, Dimitrov I, Sherry AD, Malloy CR. Composition of adipose tissue and marrow fat in humans by 1H NMR at 7 Tesla. *J Lipid Res* 2008;49: 2055–2062.
 38. Hamilton G, Schlein AN, Middleton MS, et al. In vivo triglyceride composition of abdominal adipose tissue measured by 1 H MRS at 3T. *J Magn Reson Imaging* 2017;45:1455–1463.
 39. Phinney SD, Stern JS, Burke KE, Tang AB, Miller G, Holman RT. Human subcutaneous adipose tissue shows site-specific differences in fatty acid composition. *Am J Clin Nutr* 1994;60:725–729.
 40. Gruetter R, Boesch C. Fast, noniterative shimming of spatially localized signals. in vivo analysis of the magnetic field along axes. *J Magn Reson* 1992;96:323–334.
 41. Juchem C, Umesh Rudrapatna S, Nixon TW, de Graaf RA. Dynamic multi-coil technique (DYNAMITE) shimming for echo-planar imaging of the human brain at 7 Tesla. *Neuroimage* 2015;105:462–472.